

Regenerative similariton laser

Thibault North and Camille-Sophie Brès

Citation: *APL Photonics* **1**, 021302 (2016); doi: 10.1063/1.4945352

View online: <http://dx.doi.org/10.1063/1.4945352>

View Table of Contents: <http://scitation.aip.org/content/aip/journal/app/1/2?ver=pdfcov>

Published by the [AIP Publishing](#)

Articles you may be interested in

[A switchable and stable single-longitudinal-mode, dual-wavelength erbium-doped fiber laser assisted by Rayleigh backscattering in tapered fiber](#)

J. Appl. Phys. **118**, 103107 (2015); 10.1063/1.4930054

[Narrow linewidth low frequency noise Er-doped fiber ring laser based on femtosecond laser induced random feedback](#)

Appl. Phys. Lett. **105**, 101105 (2014); 10.1063/1.4895618

[A discretely tunable multifrequency source injection locked to a spectral-mode-filtered fiber laser comb](#)

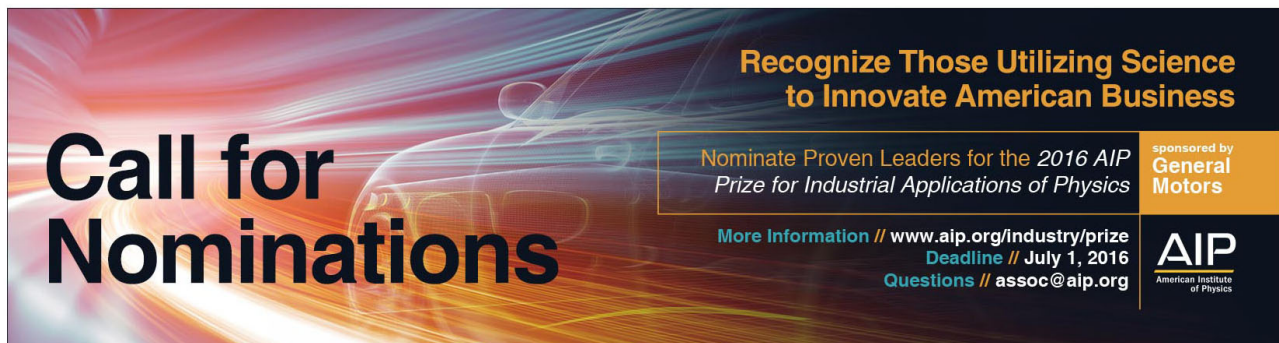
Appl. Phys. Lett. **97**, 141107 (2010); 10.1063/1.3497080

[Experimental Study of a Multicavity Fiber Laser System](#)

AIP Conf. Proc. **992**, 435 (2008); 10.1063/1.2926903

[Sub-500-fs soliton-like pulse in a passively mode-locked broadband surface-emitting laser with 100 mW average power](#)

Appl. Phys. Lett. **80**, 3892 (2002); 10.1063/1.1482143



Call for Nominations

Recognize Those Utilizing Science to Innovate American Business

Nominate Proven Leaders for the 2016 AIP Prize for Industrial Applications of Physics

More Information // www.aip.org/industry/prize
Deadline // July 1, 2016
Questions // assoc@aip.org

sponsored by General Motors

AIP
American Institute of Physics

Regenerative similariton laser

Thibault North^a and Camille-Sophie Brès

École Polytechnique Fédérale de Lausanne (EPFL), Photonic Systems Laboratory (PHOSL), STI-IEL, Station 11, CH-1015 Lausanne, Switzerland

(Received 18 November 2015; accepted 10 March 2016; published online 23 May 2016)

Self-pulsating lasers based on cascaded reshaping and reamplification (2R) are capable of initiating ultrashort pulses despite the accumulation of large amounts of nonlinearities in all-fiber resonators. The spectral properties of pulses in self-similar propagation are compatible with cascaded 2R regeneration by offset filtering, making parabolic pulses suitable for the design of a laser of this recently introduced class. A new type of regenerative laser giving birth to similaritons is numerically investigated and shows that this laser is the analog of regenerative sources based solely on self-phase modulation and offset filtering. The regenerative similariton laser does not suffer from instabilities due to excessive nonlinearities and enables ultrashort pulse generation in a simple cavity configuration. © 2016 Author(s). All article content, except where otherwise noted, is licensed under a Creative Commons Attribution (CC BY) license (<http://creativecommons.org/licenses/by/4.0/>). [<http://dx.doi.org/10.1063/1.4945352>]

Self-similar (SS) propagation of optical pulses in presence of gain, predicted in 1993 by Anderson *et al.*¹ and demonstrated in 2000 by Fermann *et al.*,² is of particular interest in the field of optical pulse propagation and fiber lasers. The unique characteristics of the similariton regime have numerous practical advantages: any pulse shape eventually converges towards a parabolic pulse,³ the output chirp is linear and only depends on the chromatic dispersion and gain, and wave-breaking is avoided.^{4,5} This eases the generation of high-energy pulses, since the seed pulse can eventually be compressed to a duration shorter than its initial transform-limit, leading to the generation of powerful sub-picosecond pulses in all-fiber configurations.^{6–10} Therefore, the optical similariton is a very attractive solution to the nonlinear Schrödinger equation in the presence of nonlinearity and gain in open-loop systems as well as ring cavities with feedback. In the theoretical and numerical results of Ref. 11 as well as the experimental works of Refs. 6, 8, and 9, a stable regime where parabolic pulses propagate in a cavity is found in a configuration that is typical of lasers mode-locked by nonlinear polarization evolution. Recently, other pulse generation mechanisms including self-similarity, dissipative solitons, adiabatic solitons, and other hybrid concepts were used to overcome the limitations of common mode-locked lasers in terms of energy.^{12–14} Such techniques limit the resonant instabilities due to the in-cavity gain and losses that the pulse undergoes. Contrary to stretched-pulse lasers which take advantage of large amounts of linear chirp to keep low peak powers in a cavity of adjusted average dispersion,¹⁵ these new configurations operate by limiting the dispersive-wave shedding and amplification in the anomalous dispersion regime or by avoiding wave-breaking in the normal regime. In these works, the authors require the presence of a component playing the role of saturable absorber. For this purpose, additive-pulse mode-locking or semiconductor saturable absorbers such as carbon nanotubes are chosen.^{16,17}

Regenerative sources (RSs), on the other hand, are a new class of pulsed lasers relying on cascaded reshaping and reamplification (2R) for pulse generation as well as saturable absorption.^{18–21} Instead of relying on a classic saturable absorber alike those mentioned above, these lasers take advantage of high amounts of accumulated $\chi^{(3)}$ nonlinear effects followed by offset band-pass filtering in order to generate ultrashort pulses in all-fiber ring configurations. RSs feature unique

^athibault.north@epfl.ch



and interesting properties such as aperiodicity as well as the ability to sustain picosecond pulses in cavities exceeding 2 km without precise control of the overall accumulated chromatic dispersion. Also, propagation in normal chromatic dispersion and spectral broadening resulting from self-phase modulation (SPM) enables nonlinear pulse compression to the femtosecond regime.^{22,23}

Here we propose a new concept for ultrashort pulse generation leveraging similariton propagation and offset filtering in a regenerative cavity configuration. Extensive numerical investigations show that a stable pulse transition to similariton is possible in presence of feedback and wavelength toggling by alternate band-pass filtering. Moreover, the proposed setup based on Raman amplification is extremely simple and does not require highly nonlinear fibers, rare-earth doped fibers, nor additional saturable absorber. Similaritons enable a wave-breaking free propagation, thereby preserving a large pulse energy and confining the power spectral density (PSD) of the pulses within a bandwidth of a few nanometers without shedding energy in the transitional state, unlike solitons.²⁴ To our knowledge, no such architecture was reported so far. Previous work by Pitois *et al.*¹⁹ briefly presents a laser architecture which includes a regenerative stage featuring similariton propagation. However, numerical simulations presented in Ref. 19 are based on a simplified model that does not take into account saturable absorption into saturable absorption, and does not show that SS propagation only is sufficient to trigger and sustain pulses. The same group also experimentally reported 2R regeneration based on optical similaritons rather than SPM and offset filtering.^{25,26} This optical signal regeneration from similaritons in an open loop suggests that an experimental implementation of the proposed regenerative similariton laser is possible. This laser may prove useful in applications for which dual-wavelength oscillation, wavelength tuning, or tunable pulse duration is desired. As for the source of Ref. 20, pulse buffering is also readily available from this cavity.

The self-pulsating laser source under study is depicted in Fig. 1. For simplicity, two Raman pumps at 1480 nm are used and modeled as to provide a flat gain in the C-band, around 1550 nm. A single pump acting backwards for one half-cavity round-trip and forwards for the other could be sufficient, as these two pumping configurations have already been investigated for self-similar propagation.^{27,28} The dispersion-shifted fiber (DSF) has realistic properties taken from Ref. 28. It has a length of 6200 m, a normal dispersion with a chromatic dispersion coefficient of $\beta_2 = 3.3 \text{ ps}^2/\text{km}$, and a nonlinear waveguide coefficient $\gamma = 1.7 \text{ W}^{-1} \text{ km}^{-1}$. A section of 800 m of single-mode fiber (SMF) is included after each filtering stage to compensate for the chirp resulting of the self-similar propagation in the DSF. Third-order dispersion is neglected,⁴ and the gain is assumed to be flat over the bandwidth 1545–1560 nm, a reasonable assumption since similaritons are robust to gain fluctuations.²⁹ The small signal Raman gain coefficient $g_0 = g_R - \alpha$ is the difference between the effective Raman gain coefficient and the fiber losses α and has a value of $1.92 \times 10^{-3} \text{ m}^{-1}$. The saturable gain is $g = P_{\text{in}} g_0 \exp[-(P_{\text{out}} - P_{\text{in}})/P_{\text{sat}}]$, with a saturation power of $P_{\text{sat}} = 15 \text{ mW}$. The band-pass filters (BPFs) spectrally have a Gaussian profile with 1 nm full-width at half-maximum (FWHM), and a spectral offset of $\Delta\Omega = 1.7 \text{ nm}$ is set between BPF₁ and BPF₂. The source self-starts from noise, and pulses build-up in the cavity, which is unidirectional except for the DSF section. In this study of the

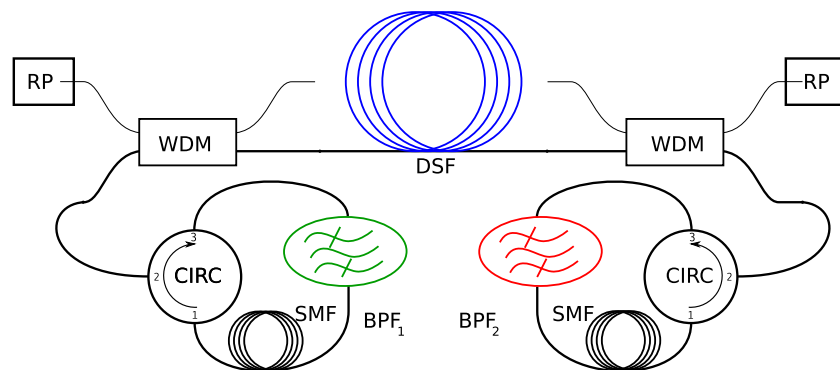


FIG. 1. Setup of the laser under study. BPF: band-pass filter, SMF: single-mode fiber, DSF: dispersion shifted fiber, CIRC: optical circulator, RP: Raman pump, WDM: wavelength division multiplexer.

cavity dynamics, no additional tap coupler is included. The power extracted via a tap coupler can be directly compensated by a gain increase. Moreover, the part of the spectrum rejected by each BPFs can also be used as source output.

Propagation in the fiber sections is modelled with the well-known split-step Fourier method,³⁰

$$\frac{\partial A}{\partial z} + \frac{g}{2}A + \frac{i}{2}\beta_2\frac{\partial^2 A}{\partial T^2} = i\gamma\left(|A|^2A + \frac{i}{\omega_0}\frac{\partial}{\partial T}(|A|^2A) - T_R A\frac{\partial|A|^2}{\partial T}\right), \quad (1)$$

where ω_0 is the central frequency, and T the time in a reference frame moving at the group velocity v_g . Self-steepening and the Raman effect are taken into account in (1) with a linear approximation with $T_R = 3$ fs. Cascaded Raman scattering is neglected in this work. It is known that the Raman effect has detrimental effects on SS.^{5,30} However the pulse powers involved here are below the Raman threshold that we estimate between 1 and 2 W, depending on the fiber parameters.³¹

As expected for a RS, pulses are aperiodically initiated from noise, and after less than 50 cavity round-trips, a steady-state is found as illustrated in Figs. 2(a) and 2(b). The inset indicates that multiple pulses can coexist in the cavity if P_{sat} is high enough. The relative delay between the pulses is random, determined by the initial amplified spontaneous emission (ASE) pattern. The RF spectrum of Fig. 2(c) corresponds to the pulse train of the inset of Fig. 2(a), typical of aperiodic sources. The pulse energy and duration depend on the steady-state gain, which dictates the self-similar propagation. The number of pulses present in the cavity follows the rules applying to RSs and therefore depends mostly on the saturation power of the amplifier as well as the relative positions of the BPFs. Each BPF transmits 18% of the pulse energy, which exceeds the efficiency of RSs based solely on SPM spectral broadening and offset filtering³² with similar bandwidths.

In order to assess that the pulses sustained in the cavity have reached a parabolic shape temporally and spectrally, their proximity to a parabolic shape is measured. The temporal misfit parameter is defined by the difference between the pulse intensity $|\Psi|^2$ profile in the temporal domain and an ideal parabolic pulse $|\Psi_{\text{fit}}|^2$,³³

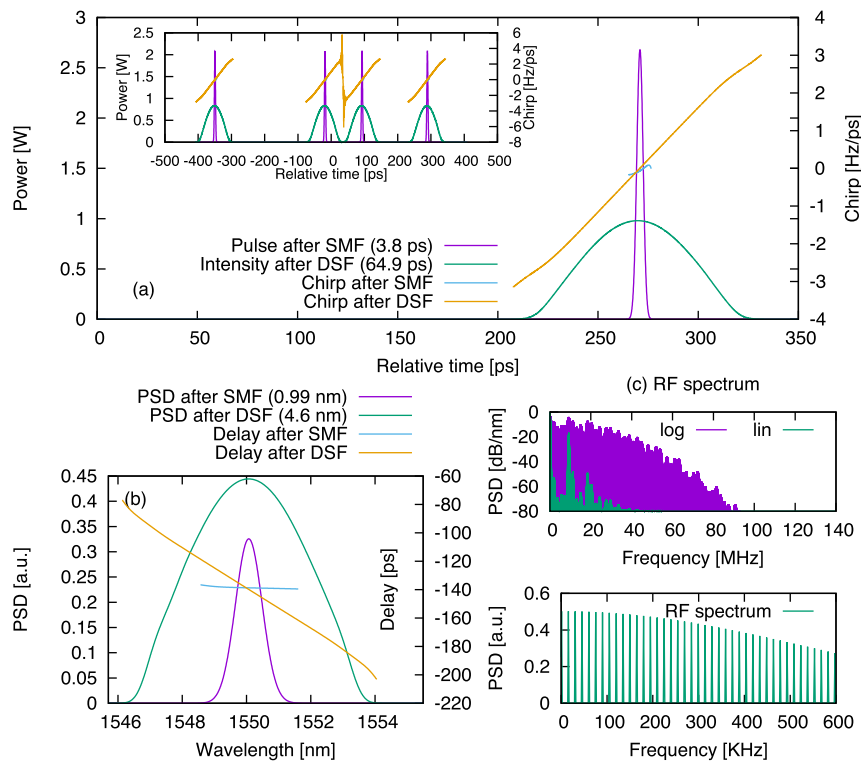


FIG. 2. Source operation in steady state at cavity round-trip 50 in the (a) temporal and (b) spectral domains. Inset: randomly spaced multiple pulses when the saturation power is increased three times. (c): RF spectrum of the pulse train of (a), inset.

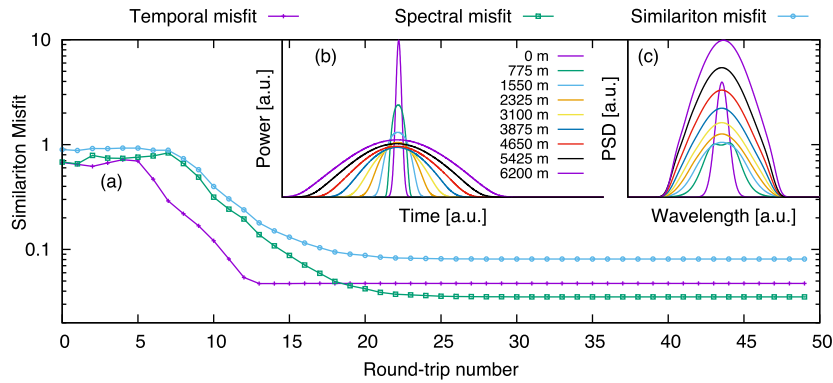


FIG. 3. (a) Pulse convergence towards similaritons for the first 50 cavity round-trips, when self-starting from noise. (b) and (c) Steady-state temporal and spectral profiles of the pulse during their propagation in the DSF every 775 m.

$$M_t^2 = \frac{\int [|\Psi|^2 - |\Psi_{\text{fit}}|^2]^2 dt}{\int |\Psi|^4 dt}. \quad (2)$$

Analogously, we define the spectral misfit parameter M_s^2 from (2), but with the power spectral density $|\hat{\Psi}(\omega)|^2$ of the pulse and its ideal fit $|\hat{\Psi}(\omega)_{\text{P-fit}}|^2$. Finally, we define the overall similariton misfit as

$$M = 1 - (1 - M_t)(1 - M_s) = M_t + M_s - M_t M_s. \quad (3)$$

The build-up of pulses from ASE is illustrated by the decrease of the misfit parameters defined above in Fig. 3(a). Figs. 3(b) and 3(c) indicate that the pulse passes through a SPM amplification regime³³ before reaching SS propagation. Nevertheless, the final pulse profile at the output of the fiber in steady-state regime is parabolic, and both the temporal and spectral misfits exhibit small values. In Fig. 4, the temporal and spectral features of the pulse in their steady-state propagation in the cavity are illustrated for round-trip number 50. The spectral bandwidth and temporal pulse duration increase together when propagating in the DSF, towards a SS regime. Band-pass filtering selects a spectral slice of the linearly chirped pulse, thereby decreasing its duration at the same time. Dispersion compensation in the SMF with anomalous dispersion compresses the pulse, increasing its peak power by a factor of four, but also resetting the chirp and permitting faster convergence towards a SS state. Without compensating the dispersion, the latter accumulates and slows down the formation of a parabolic pulse in the DSF, and the source does not self-start. Indeed, similariton

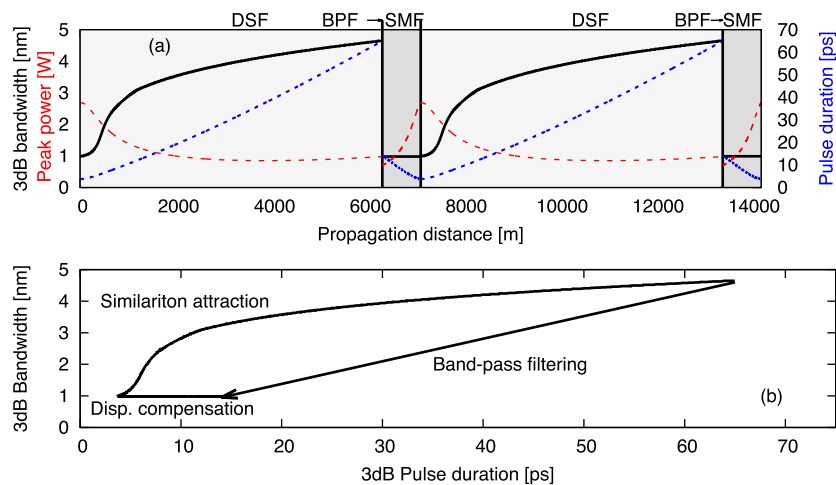


FIG. 4. Evolution of the pulse in the cavity. (a) Pulse bandwidth (solid), bandwidth (dashed), peak power (dotted). (b) Time and bandwidth evolution for a cavity round-trip.

propagation in this configuration is only at an early stage, as indicated by Fig. 4(a). With gain and dispersion parameters tuned, faster convergence toward a similariton would allow resetting the input chirp as well as providing a constant output chirp, depending only on the gain and dispersion without additional SMF. An overview of the pulse duration and bandwidth during one cavity round-trip is provided in Fig. 4(b). References 33 and 34 point out the influence of an initial chirp on the transitional propagation dynamics. In the regenerative feedback loop under study, the accumulated Raman gain is dynamically defined by the energy circulating inside the cavity. For the steady-state gain, a propagation towards SS is initiated from the seed pulse. Depending on its chirp, the pulse spectrum during propagation in the DSF may undergo a smooth change towards a parabolic profile, as depicted earlier in Fig. 3(c), or via the generation of sidebands initiated by SPM. Because the gain medium is finite, for a given seed pulse bandwidth and a variable chirp, not all pulses reach the same proximity to a similariton. Hence, the energy transmitted after one regeneration stage varies, as well as the similariton misfit parameter of (3), as illustrated in Figure S1 of the supplementary material.³⁵ The similariton laser operates by finding a steady-state for which the seed pulse carries a chirp which is low enough to allow approaching self-similarity within the fiber length. This steady-state does not necessarily correspond to the pulse energy and chirp that maximizes the energy transmission in the open-loop configuration.

But the critical function defining whether the source self-starts and converges to a well-defined state is the shape of the energy transfer function (ETF), which must give birth to saturable absorption. In case of similariton regeneration, the input energy defines whether the pulse will be able to reach a SS asymptotic regime or not. The transfer function relating the output energy to the input energy must therefore feature an inflection point, such that the low energy pulses continuously lose power at the filtering stage, while the high energy pulses stabilize towards a unique energy value, as depicted in Fig. 5(a). Fig. 5(b) illustrates the actual transmission at each regeneration stage for an input pulse corresponding to the stable solution of the laser under study ($\Delta\Omega = 1.7$ nm), as well as for $\Delta\Omega = 2$ nm and 3 nm. The larger the filter offset, the more the ETF discriminates low energies, but larger values of $\Delta\Omega$ also require a larger gain to sustain pulses in the cavity. In Fig. 5(c), the ETF shows that all pulses of energies above $P_1 \approx 60$ pJ will converge to that value, as well as the ones of energies larger than $P_2 \approx 30$ pJ. Pulses with energies lower than P_2 are discarded by the regenerator. The line $E_{out} = E_{in}$ intersects the ETF in two points, P_1 being a stable solution, while P_2 is unstable. Fig. 5(d) corroborates this fact by showing that the ETF resulting of multiples passes through

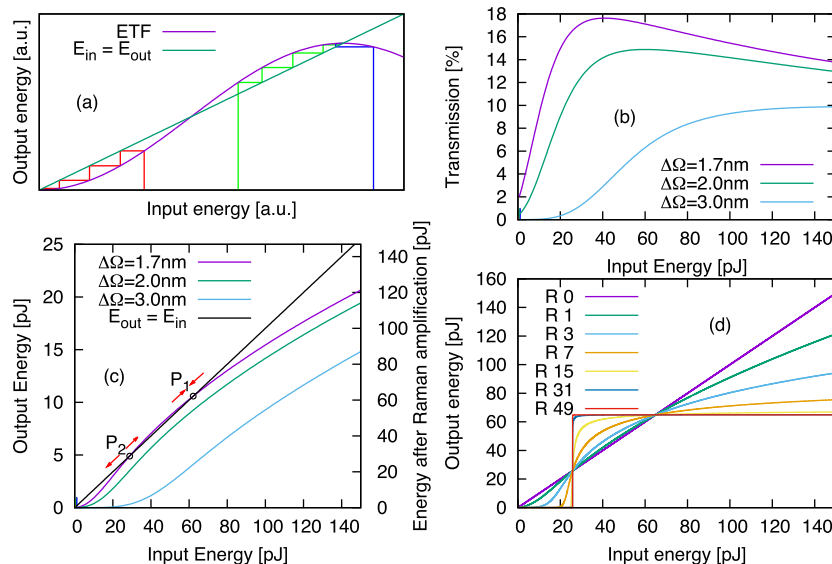


FIG. 5. (a) Typical shape of an adequate energy transfer function (ETF). (b) Transmission of a regenerator as a function of the input energy. (c) Actual ETF: pulse of low energy (red) is discarded. Pulse of high energy (green, blue) converges towards a single solution. (d) Cascaded energy transfer function after 0, 1, 3, 7, 15, 31, and 49 regenerators.

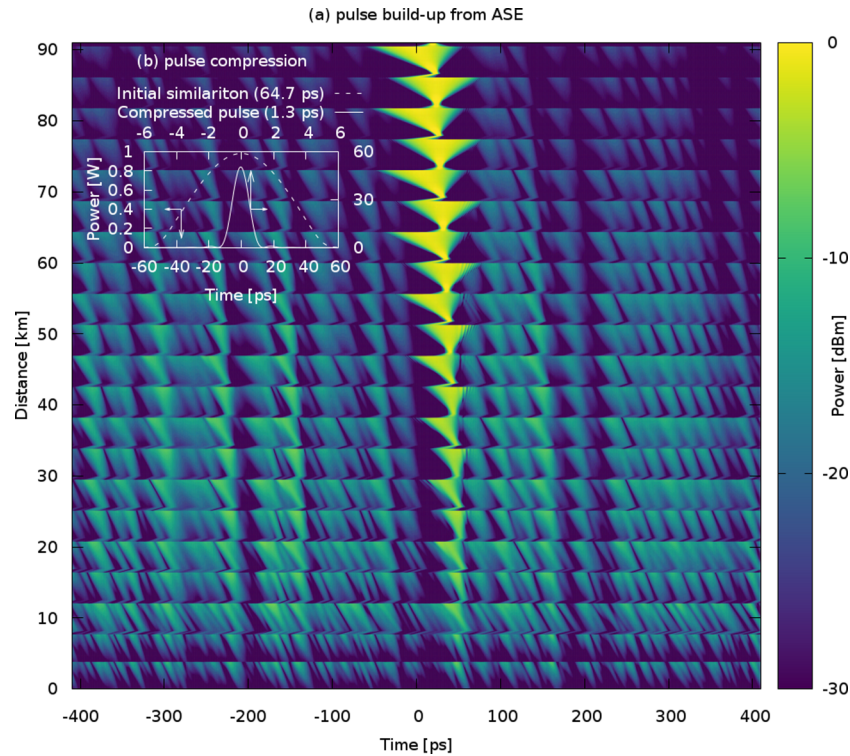


FIG. 6. (a) Pulse buildup for the first 13 cavity round trips. (b) Steady-state similariton and compressed pulse by chromatic dispersion compensation.

the regeneration stages leads to a step function which forbids the existence of pulses with other energies. In Fig. 6(a), the temporal pattern of the signal is depicted for the first 13 cavity round-trips and illustrates the competition and collisions leading to a steady-state. Because the filtered spectrum is initially parabolic and features no oscillations, it seems that no multiple limit cycles leading to pulses of different peak power are supported by the cavity, unlike regenerative sources relying on cascaded Mamyshev regeneration.^{19,32} Pulse compression is shown in Fig. 6(b). From steady-state operation, dispersion compensation decreases the pulse duration down to 1.3 ps, a compression ratio of 50 \times . This duration is 2.75 \times smaller than that of a transform-limited Gaussian pulse of 1 nm of bandwidth and corresponds to the minimal time-bandwidth product of 0.73 for the compression of chirped parabolic pulses.

In conclusion, we have numerically reported a new architecture of RS based on similariton propagation. A simple experimental setup enables the generation of picosecond pulses, linearly chirped, which can be recompressed in a dispersive medium. Accessing sub-picosecond operation can be achieved by further similariton propagation to broaden the spectrum above 5.8 nm at 3 dB. This architecture has several advantages with respect to previous reports of regenerative sources:^{21,22} wave-breaking is avoided, the filtering stage preserves a large amount of spectral components, and the source is not chaotic. It is expected that larger BPFs, discarding less spectral components, lead to a better efficiency without compromise on the pulse shape, contrary to regenerative sources solely based on SPM.²³ In future work, the influence of cascaded Raman scattering could be investigated, as well as the potential of this architecture to operate with rare-earth doped fibers rather than with Raman pumping. We believe that an experimental implementation of such a cavity is possible based on the numerical results presented in this work with a Raman pump or with another normally dispersive gain medium.

¹ D. Anderson, M. Desaix, M. Karlsson, M. Lisak, and M. L. Quiroga-Teixeiro, *J. Opt. Soc. Am. B* **10**, 1185–1190 (1993).

² M. E. Fermann, V. I. Kruglov, B. C. Thomsen, J. M. Dudley, and J. D. Harvey, *Phys. Rev. Lett.* **84**, 6010–6013 (2000).

³ V. I. Kruglov, A. C. Peacock, J. D. Harvey, and J. M. Dudley, *J. Opt. Soc. Am. B* **19**, 461–469 (2002).

- ⁴ J. M. Dudley, C. Finot, D. J. Richardson, and G. Millot, *Nat. Phys.* **3**, 597–603 (2007).
- ⁵ C. Finot, J. Dudley, B. Kibler, D. Richardson, and G. Millot, *IEEE J. Quantum Electron.* **45**, 1482–1489 (2009).
- ⁶ F. O. Ilday, J. R. Buckley, W. G. Clark, and F. W. Wise, *Phys. Rev. Lett.* **92**, 213902 (2004).
- ⁷ C. Billet, J. Dudley, N. Joly, and J. Knight, *Opt. Express* **13**, 3236–3241 (2005).
- ⁸ B. Oktem, C. Ülgüdür, and F. Ömer Ilday, *Nat. Photonics* **4**, 307–311 (2010).
- ⁹ C. Agueraray, D. Méchin, V. Kruglov, and J. D. Harvey, *Opt. Express* **18**, 8680–8687 (2010).
- ¹⁰ A. Chong, L. G. Wright, and F. W. Wise, *Rep. Prog. Phys.* **78**, 113901 (2015).
- ¹¹ V. I. Kruglov, D. Méchin, and J. D. Harvey, *Phys. Rev. A* **81**, 023815 (2010).
- ¹² L. M. Zhao, D. Y. Tang, and J. Wu, *Opt. Lett.* **31**, 1788–1790 (2006).
- ¹³ C. Lecaplain, M. Baumgartl, T. Schreiber, and A. Hideur, *Opt. Express* **19**, 26742–26751 (2011).
- ¹⁴ A. Bednyakova and S. K. Turitsyn, *Phys. Rev. Lett.* **114**, 113901 (2015).
- ¹⁵ K. Tamura, E. Ippen, H. Haus, and L. Nelson, *Opt. Lett.* **18**, 1080–1082 (1993).
- ¹⁶ H. Haus, E. Ippen, and K. Tamura, *IEEE J. Quantum Electron.* **30**, 200–208 (1994).
- ¹⁷ S. Y. Set, H. Yaguchi, Y. Tanaka, and M. Jablonski, *J. Lightwave Technol.* **22**, 51 (2004).
- ¹⁸ S. Pitois, C. Finot, and L. Provost, *Opt. Lett.* **32**, 3263–3265 (2007).
- ¹⁹ S. Pitois, C. Finot, L. Provost, and D. Richardson, *J. Opt. Soc. Am. B* **25**, 1537–1547 (2008).
- ²⁰ M. Rochette, L. R. Chen, K. Sun, and J. Hernandez-Cordero, *IEEE Photonics Technol. Lett.* **20**, 1497–1499 (2008).
- ²¹ T. North, A. Al-kadry, and M. Rochette, *IEEE J. Sel. Top. Quantum Electron.* **20**, 1–7 (2014).
- ²² K. Sun, M. Rochette, and L. R. Chen, *Opt. Express* **17**, 10419–10432 (2009).
- ²³ T. North and M. Rochette, *Opt. Lett.* **39**, 174–177 (2014).
- ²⁴ S. Kelly, *Electron. Lett.* **28**, 806–807 (1992).
- ²⁵ P. Mamyshev, in *24th European Conference on Optical Communication* (IEEE, 1998), Vol. 1, pp. 475–476.
- ²⁶ C. Finot, S. Pitois, and G. Millot, *Opt. Lett.* **30**, 1776–1778 (2005).
- ²⁷ C. Finot, G. Millot, C. Billet, and J. Dudley, *Opt. Express* **11**, 1547–1552 (2003).
- ²⁸ K. Hammani, S. Boscolo, and C. Finot, *J. Opt.* **15**, 025202 (2013).
- ²⁹ V. I. Kruglov, A. C. Peacock, J. M. Dudley, and J. D. Harvey, *Opt. Lett.* **25**, 1753–1755 (2000).
- ³⁰ G. Agrawal, “Nonlinear fiber optics,” in *Optics and Photonics* (Academic Press, 2007).
- ³¹ C. Headley and G. Agrawal, *Raman Amplification in Fiber Optical Communication Systems* (Academic Press, 2005).
- ³² T. North and M. Rochette, *J. Lightwave Technol.* **31**, 3700–3706 (2013).
- ³³ C. Finot, F. Parmigiani, P. Petropoulos, and D. Richardson, *Opt. Express* **14**, 3161–3170 (2006).
- ³⁴ C. Finot and L. Wu, *J. Nonlinear Opt. Phys. Mater.* **18**, 709–721 (2009).
- ³⁵ See supplementary material at <http://dx.doi.org/10.1063/1.4945352> for figure and its description.